

The Disk and Environment of a Young Altair Analog: SAO 206462

C.A. Grady^{1,2}, G. Schneider³, M.L. Sitko^{4,5,6}, G.M. Williger^{7,8},
K. Hamaguchi^{9,2}, S.D. Brittain¹⁰, K. Ablordeppey⁵, D. Apai³,
L. Beerman⁵, W.J. Carpenter⁵, K.A. Collins^{7,11}, M. Fukagawa¹²,
H.B. Hammel^{4,6}, Th. Henning¹³, D. Hines⁴, R. Kimes⁵, D.K. Lynch^{14,6},
R. Pearson^{14,6}, R.W. Russell^{14,6}, F. Ménard¹⁵, M. Silverstone^{1,3},
P. Smith³, M. Troutman¹⁰, D. Wilner¹⁶, B. Woodgate¹⁷

Abstract. Proto-planetary and transitional disks which are detected in scattered light provide a critical test of the interpretation of circumstellar disks based on the IR spectral energy distribution (SED) alone. The disk inclination to the line-of-sight, outer radius, and surface brightness (SB) maps or radial SB distributions provided by spatially resolved imaging remove most of the degeneracies inherent in fitting IR SEDs without such observational constraints. We have imaged the disk of SAO 206462 (HD 135344B) in 1.1 and 1.6 μ m scattered light with HST/NICMOS and can trace the essentially face-on disk out to 1.05". The cavity detected in sub-mm observations lies entirely under the NICMOS coronagraphic spot, a result consistent with the SED fitting if the star is at $d=140$ pc. The SED had previously been classified as a Meeus Group I SED and interpreted as arising in a flared disk. Neither the 1.1 nor the 1.6 μ m radial surface brightness profiles are consistent with a flared disk. A FUSE FUV spectrum demonstrates the presence of excess light in this system, confirming the accretion rate estimated from Bry. Collectively, these data strengthen the interpretation of this system as a transitional disk.

Keywords: stars: protoplanetary disks, stars: transitional disks, stars: rotation, stars: accretion, stars: individual: SAO 206462

PACS: 97.82.Jw, 97.21.+a, 97.10.kc, 95.85.jq

INTRODUCTION

For the vast majority of protoplanetary and transitional disks detected by the *Spitzer* Space Telescope, knowledge of the disk is based on modeling of the infrared spectral energy distribution (SED) without spatially resolved images. Despite the known degeneracy between disk inclination and grain size effects (Chiang & Goldreich 1999), the SEDs have been grouped into those which can be fit as a powerlaw (Meeus group II),

¹ Eureka Scientific, ² Goddard Space Flight Center, ³ Steward Observatory, The University of Arizona, ⁴ Space Science Institute, ⁵ University of Cincinnati, ⁶ Visiting Astronomer, NASA Infrared Telescope Facility, ⁷ University of Louisville, ⁸ The Johns Hopkins University, ⁹ CRESST and University of Maryland, Baltimore County, ¹⁰ Clemson University, ¹¹ supported by the Kentucky Space Grant Consortium and NASA, ¹² Osaka University, ¹³ Max-Planck-Institut für Astronomie, ¹⁴ The Aerospace Corporation, ¹⁵ Laboratoire d'Astrophysique de Grenoble, ¹⁶ Harvard-Smithsonian Center for Astrophysics, ¹⁷ NASA's Goddard Space Flight Center

and those with an additional blackbody component (Meeus group I). Group I disks are interpreted as flared disks with well-mixed gas and dust, while the Group II disks are interpreted as disks with grain growth and settling toward the disk mid-plane (Meeus et al. 2001; Dullemond & Dominik 2004a,b). Those disks lacking dust radiating at near-IR wavelengths have been termed "transitional disks" (Najita et al. 2007).

The interpretation of these SEDs can be checked if the disk can be detected in scattered light, such as can be provided by HST coronagraphic observations. Scattered-light detections of the disk provide a direct measure of disk inclination, outer radius, and the dependence of the disk surface brightness on radius, while additional constraints are available if the disk is detected at 2 or more wavelengths. One such disk is associated with the Herbig F star SAO 206462 (HD 135344B).

HST/NICMOS CORONAGRAPHIC IMAGERY

We conducted HST/NICMOS imaging of SAO 206462 on 2005 March 24 UT with NICMOS camera 2 coronagraphy. The star was imaged in 2 independent observation sets obtained at 2 HST roll angles separated by 29.9° . The disk was detected in both observation sets at $1.1\mu\text{m}$ after subtracting a suite of point spread function (PSF) template observations matched to the J-H color of the star. At $1.6\mu\text{m}$, the disk had previously been reported as a non-detection (Augereau et al. 2001). We recover the disk out to $0.9''$ by using a contemporary, red PSF template star as close in H-K color to SAO 206462 as feasible (fig. 1). The disk is not detected at $1.1\mu\text{m}$ after roll-differencing, which would reveal an azimuthally asymmetric disk, indicating $i \leq 20^\circ$. The disk imagery is in good agreement with the sub-millimeter data (Pontoppidan et al. 2008) and modeling of the CO emission (Dent et al. 2005), but not the analysis of Doucet et al. (2006).

Flared disks are expected to have relatively shallow radial surface brightness profiles, with $SB \propto r^{2-2.5}$, while disks with significant stratification due to grain growth should have disks with steeper radial surface brightness profiles. At $1.1\mu\text{m}$, we find $r^{-9.6}$ for the azimuthally-mediated SB. We do find a roll-over in the surface brightness data at $1.1\mu\text{m}$ near $0.6''$, which is not coincident with the cavity noted in the sub-millimeter imagery. The outer disk ($0.6 \leq r \leq 0.7''$) is bluer than the color of the star, while the zone from $0.45 \leq r \leq 0.6''$ approaches the stellar color, indicating scattering by larger grains than in the outer disk (fig. 2). The IR SED and disk surface brightness data can be fit using the Whitney Monte Carlo Radiative Transfer Code only if the disk is anti-flared from $0.3''$ outward. The constraints provided by the disk outer radius and system inclination further exclude SED fits with ISM-like grains (either with or without icy mantles), requiring significant grain growth and settling throughout the disk.

THE DISTANCE TO SAO 206462, AND THE STAR ITSELF

Brown et al. (2007) find that the inner rim of the outer disk lies 45 AU from the star. The NICMOS imagery indicates that any such structure must lie interior to $0.3''$, in the region occulted by the coronagraphic spot. Two distances to SAO 206462 have been used in the literature: $d=84$ pc (Sylvester et al. 1996) and $d=140$ pc (van Boekel et al. 2005).

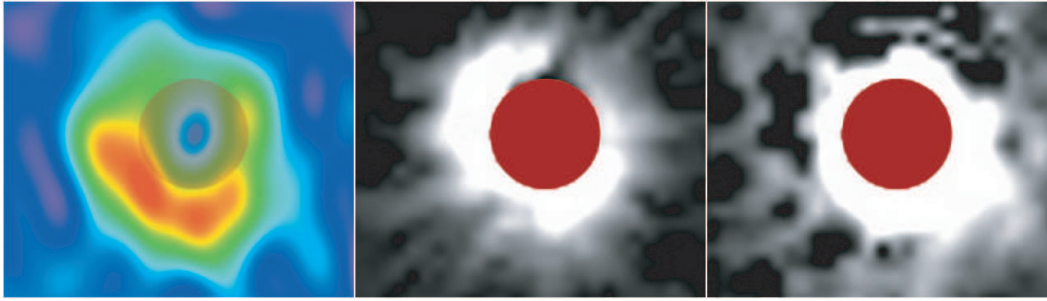


FIGURE 1. The disk of SAO 206462 in the sub-millimeter continuum (Pontoppidan et al. 2008). Middle and Right: Near-IR coronagraphic images at 1.1 and 1.6 microns, respectively. All three images at the same spatial scale and orientation (North up east left). The red circle represents the $r=0.3''$ region obscured by the NICMOS coronagraph, and is overlaid in light gray on the sub-mm image.

At 84 pc, 45 AU corresponds to $0.53''$, exterior to the ring seen in the sub-millimeter continuum imagery. This radius also lies at a location where the disk is firmly detected and featureless in scattered light. For $d=140$ pc, the predicted rim location coincides with the inner edge of the sub-millimeter ring and lies inside the NICMOS spot. We therefore adopt $d=140$ pc for SAO 206462.

With $d=140$ pc, SAO 206462's age is 8 ± 4 Myr (van Boekel et al. 2005). Like other, coeval stars such as TW Hya, SAO 206462 continues to accrete material at $\dot{M}=5 \times 10^{-9} M_{\odot} \text{ yr}^{-1}$ (seen at Bry (Garcia Lopez et al. 2006), and in the FUV (Grady et al. 2009)). This accretion rate suggests that SAO 206462's disk is not pre-transitional, as suggested by Brown et al. (2007), but is already a transitional disk system. With this age estimate, also we find that SAO 206462, at $1.7 M_{\odot}$, will be a mid- to late-A star when it reaches the ZAMS. Combining the inclination data with $v \sin i$ (Dunkin et al. 1997), we find $v_{eq} \approx 360$ km/s, making SAO 206462 a young Altair analog. The presence of rapid rotation suggests, that despite being a late-type star throughout its PMS evolution to date, the star has not experienced significant magnetic braking. We anticipate that the magnetic field of SAO 206462 may more closely resemble early- to mid-A Herbig Ae stars than that of classical T Tauri stars.

ACKNOWLEDGMENTS

This study has made use of HST coronagraphic imagery obtained as part of HST-GO-10177, supplemented with archival data, and FUV imagery from HST-GO-10864. This study also made use of FUSE FUV spectral data obtained as part of FUSE Legacy program E510. This work was supported under The Aerospace Corporation's Independent Research and Development Program. CAG is also supported as part of the Astrophysics Data Program under NASA Contract NNH06CC28C to Eureka Scientific, and HST-GO-10177.02-A. GS is supported under HST-GO-10177.01. MLS is supported through the NASA Origins of Solar Systems Program NAG5-9475 and NAG5-13242. K.H. is supported by the NASA Astrobiology Program under CAN 03-OSS-02. S.D.B. acknowledges support for this work from the National Science Foundation under grant number AST-0708899.

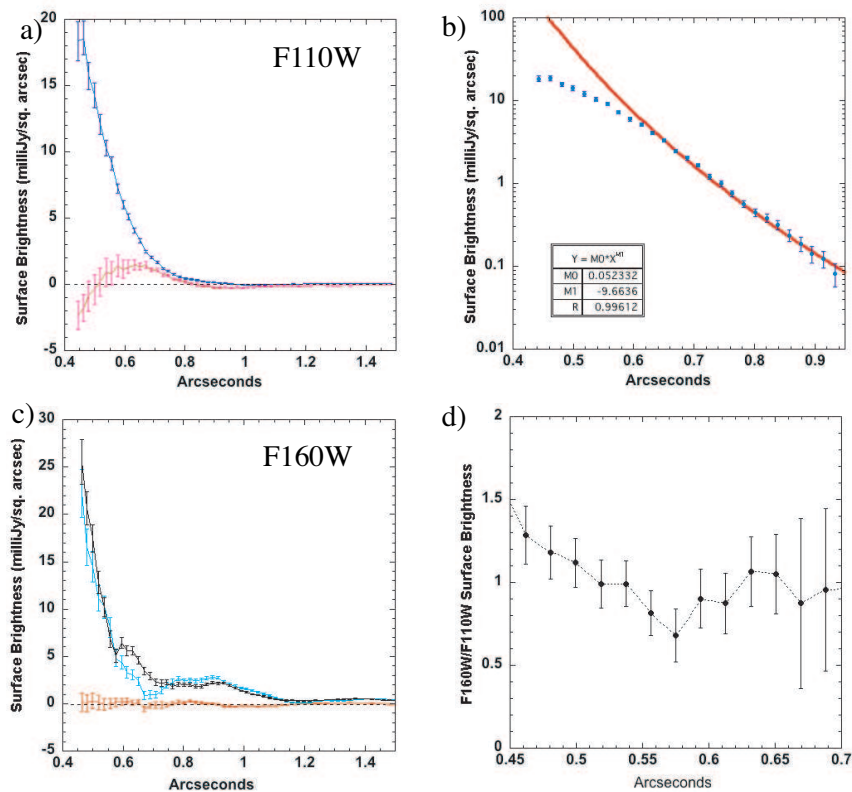


FIGURE 2. Azimuthally-averaged radial surface brightness data for SAO 206462. a) $1.1\mu\text{m}$, b) fit to $1.1\mu\text{m}$ SB data, c) $1.6\mu\text{m}$, d) ratio of the $1.6/1.1\mu\text{m}$ data. Gray scattering should have a color similar to the star or $J-H=1.5$.

REFERENCES

1. Augereau, J.-C., Lagrange, A.M., Mouillet, D., Ménard, F. 2001, *A&A*, **365**, 78-89.
2. Brown, J. M. et al. 2007, *ApJ*, **664**, 107-110.
3. Chiang, E.I., & Goldreich, P., 1999, *ApJ* **519** 279-284.
4. Dent, W.R.F., Greaves, J.S., & Coulson, I.M. 2005, *MNRAS*, **359**, 663-676.
5. Doucet, C., Pantin, E., Lagage, P.O., Dullemond, C.P. 2006, *A&A* **460**, 117-124.
6. Dullemond, C.P.E., & Dominik, C. 2004a, *A&A*, **417**, 159-168.
7. Dullemond, C.P.E., & Dominik, C. 2004b, *A&A*, **421**, 1075-1086.
8. Dunkin, S.K., Barlow, M.J., Ryan, S.G. 1997, *MNRAS*, **290**, 165-185.
9. Garcia Lopez, R., Natta, A., Testi, L., Habart, E. 2006, *A&A*, **459**, 837-842.
10. Grady, C.A. et al. 2009, *ApJ* (submitted).
11. Meeus, G., Waters, L.B.F.M., Bouwman, J., van den Ancker, M.E., Waelkens, C., Malfait, K. 2001, *A&A*, **365**, 476-490.
12. Najita, J.R., Strom, S.E., Muzerolle, J. 2007, *MNRAS*, **378**, 369-378.
13. Pontoppidan, K.M., Blake, G.A., van Dishoek, E.F., Smette, A., Ireland, M.J., Brown, J. 2008, *ApJ*, **684**, 1323-1329.
14. Sylvester, R.J., Skinner, C.J., 1996, *MNRAS*, **283**, 457-470.
15. van Boekel, R., Min, M., Waters, L.B.F.M., de Koter, A., Dominik, C., van den Ancker, M.E., Bouwman, J. 2005, *A&A*, **437**, 189-208.